energies

MDPI

Article

Multi-Objective Optimization Design for Cold-Region Office Buildings Balancing Outdoor Thermal Comfort and Building Energy Consumption

Fei Guo, Shiyu Miao, Sheng Xu, Mingxuan Luo, Jing Dong * and Hongchi Zhang *

School of Architecture and Fine Art, Dalian University of Technology, Dalian 116024, China; guofei@dlut.edu.cn (F.G.); miaoshiyu@mail.dlut.edu.cn (S.M.); xusheng@mail.dlut.edu.cn (S.X.); 32216047@mail.dlut.edu.cn (M.L.)

* Correspondence: jdong@dlut.edu.cn (J.D.); zhanghc@dlut.edu.cn (H.Z.)

Abstract: Performance parameters and generative design applications have redefined the human–machine collaborative relationship, challenging traditional architectural design paradigms and guiding the architectural design process toward a performance-based design transformation. This study proposes a multi-objective optimization (MOO) design approach based on performance simulation, utilizing the Grasshopper-EvoMass multi-objective optimization platform. The Non-dominated Sorting Genetic Algorithm II (NSGA-II) is applied to coordinate two performance metrics—outdoor thermal comfort and building energy loads—for the multi-objective optimization of architectural design. The results indicate that (1) a performance-based multi-objective optimization design workflow is established. Compared to the baseline design, the optimized building form shows a significant improvement in performance. The Pareto optimal solutions, under 2022 meteorological conditions, demonstrate an annual energy efficiency improvement of 16.55%, and the outdoor thermal neutrality ratio increases by 1.11%. These results suggest that the optimization approach effectively balances building energy loads and outdoor thermal comfort. (2) A total of 1500 building form solutions were generated, from which 16 optimal solutions were selected through the Pareto front method. The resulting Pareto optimal building layouts provide multiple feasible form configurations for the early-stage design phase.

Keywords: multi-objective optimization; building energy consumption; outdoor thermal comfort; office buildings

Academic Editor: Francesco Minichiello

Received: 2 December 2024
Revised: 20 December 2024
Accepted: 22 December 2024
Published: 27 December 2024

Citation: Guo, F.; Miao, S.; Xu, S.; Luo, M.; Dong, J.; Zhang, H. Multi-Objective Optimization Design for Cold-Region Office Buildings Balancing Outdoor Thermal Comfort and Building Energy Consumption. *Energies* **2025**, *18*, 62. https://doi.org/10.3390/en18010062

1. Introduction

The rapid urbanization process is profoundly altering the urban climate, with extreme weather events becoming more frequent, the urban heat island effect intensifying, and carbon emissions rising globally [1]. Poor environmental conditions pose significant threats to public health. Against the backdrop of climate and energy concerns, scholars worldwide have begun to focus on urban form studies based on multiple performance indicators [2]. In the cold regions of northeast China, where winters are long and harsh, thermal comfort significantly impacts the actual experience. Office buildings need to strike a balance between functional demands, sustainability, and comfort. Multi-objective optimization has become an effective tool [3], capable of simultaneously balancing various performance metrics and adapting flexibly to external meteorological conditions.

In recent years, generative design has developed rapidly. The application of performance parameters and generative design has redefined the human–machine collaborative relationship, breaking through traditional architectural design paradigms and guiding the architectural design process toward a performance-based design transformation [4]. As an iterative algorithm that coordinates multiple parameters, multi-objective optimization is suitable for meeting the need to coordinate various goals in architectural design, and it is crucial when balancing conflicting objectives [5–7]. This study selects a typical office building in Dalian as the research sample and analyzes the influence patterns of multiple factors through multi-objective optimization of architectural forms. The research aims to explore strategies for performance-based design in cold regions and provide methods and theoretical references for architects in the early-stage design of building forms.

Integrating multi-objective optimization methods into the conceptual phase of architectural design helps address the complex goals of achieving optimal energy efficiency while enhancing thermal comfort. Current research on the application of multi-objective optimization in architectural design can be categorized into three main areas. (1) From the perspective of green buildings, research on multi-objective optimization design coordinates multiple performance indicators (such as acoustics, lighting, and thermal properties in building physics). Over the past decade, researchers in building performance have focused on the role of artificial intelligence technologies in shaping architectural forms, conducting extensive work in underlying algorithms, theoretical methods, and engineering practices [5,8–10]. Architectural designers have applied multi-objective optimization to various performance metrics. In 2016, Delgarm N. et al. [11] optimized building energy consumption and indoor thermal comfort using the Multi-objective Artificial Bee Colony (MOABC) algorithm. In 2021, Deb K. et al. [12] optimized materials for residential buildings in cold regions, targeting building life cycle assessment (LCA) costs and CO2 emissions. In 2022, Jingjin Li et al. [13] conducted multi-objective optimization for a residential area in Nanjing, using three volumetric combinations (horizontal, vertical, and hybrid) as variables, targeting the floor area ratio and solar radiation. In 2024, Xian Zhang et al. [14] applied the MOPSO algorithm to optimize indoor spaces, with objectives including visual effects and energy efficiency. (2) From the perspective of urban design, multi-objective optimization is applied at various scales (building, block, and city levels). Multi-objective optimization is employed across multiple design scales (city—block—building—room—component). In 2022, S. Mirzabeigi et al. [15] proposed a multi-objective optimization framework for urban block-scale design using parametric design and energy consumption simulations. In 2024, Maksoud A. et al. [16] studied urban block optimization, coordinating solar radiation intensity with flood resilience. In 2024, Abdul Mateen Khan et al. [17] used design–build simulations combined with machine learning methods (LGBM and LIME) to predict and optimize the energy efficiency of building units, achieving energy savings and reduced carbon emissions through multi-objective optimization (MOO). In 2024, Juan Gamero Salinas et al. [18] explored multi-objective optimization to balance the minimization of indoor overheating time and the maximization of useful daylight, focusing on multiple rooms within a building. (3) From the perspective of architectural form, research focuses on generating combinations of forms based on multiple building performance indicators through multi-objective optimization. In 2022, Hankun Lin et al. [19] developed a coupled simulation method using tools such as Ansys Fluent, Ladybug, and Honeybee to simulate the shading and wind effects of green facades. Regarding architectural form exploration, research has primarily concentrated on the early design phase of overall building form exploration. In 2023, Yu Li et al. [20] applied the multi-material bi-directional evolutionary structural optimization (BESO) method to design the "Xiong'an Wing" large cantilever core structure, improving the practical application of multi-material BESO methods in large-

scale building designs. In 2024, Younes Noorollahi et al. [21] demonstrated the significant role of climate conditions in optimizing building energy use by studying design parameters such as building orientation, shading parameters, insulation thickness, temperature set points, window-to-wall ratio, and roof insulation thickness.

The evaluation systems for the built environment are rich and diverse, with outdoor thermal comfort and building energy load both being criteria for assessing the built environment. For cold regions, the outdoor environment in winter is harsh and often uncomfortable, necessitating improvements in the built environment. Moreover, in response to the societal call for low carbon emissions, office buildings should consider how to reduce operational energy loads during the design phase. It is noteworthy that outdoor thermal comfort and building energy load are interrelated, and with a reasonable architectural layout, it is possible to coordinate these two evaluation indicators simultaneously. Therefore, this study uses outdoor thermal comfort and building energy load as two evaluation indicators, and based on these, formulates objective functions. It employs multi-objective optimization methods to explore architectural forms.

Based on the above background, current research on the application of multi-objective optimization in architectural design still has several limitations. (1) Limited scope of building types for optimization. Research primarily focuses on residential buildings, given their higher frequency of use. However, there is a lack of multi-objective optimization design studies for office buildings, especially office parks. (2) Optimization objectives need further refinement. There are few studies that standardize the treatment of outdoor thermal comfort and energy load. Existing research often uses default program methods to balance various performance metrics, applying trade-off factors to standardize multiple performance indicators, thus enabling better coordination of optimization objectives. (3) Few integrated workflows for multi-objective optimization and generative design. Current multi-objective optimization research typically focuses on idealized models, leading to results that are combinations of permutations rather than generating new design solutions. Parametric generative design addresses this gap, and integrating generative design with multi-objective optimization can better guide architects in early-stage form generation.

This study aims to investigate multi-objective optimization design for office parks in cold regions, focusing on coordinating annual energy loads and outdoor thermal comfort, with an emphasis on form changes and optimization potential under multi-objective optimization conditions. The main objectives of the research are as follows. (1) To establish a broadly applicable performance-based simulation workflow (focusing on building energy loads and outdoor thermal comfort) to create a quantitative evaluation system for the built environment. (2) To perform climate and form adaptability settings for urban areas in cold regions (modifying meteorological data based on the urban heat island effect), thereby enhancing the accuracy of performance simulation workflows. (3) To explore the possibilities of architectural forms within a plot by combining multi-objective optimization with generative design under constraints such as building form parameters (floor area ratio, number of stories, enclosure degree, etc.).

The remainder of this paper is structured as follows. Section 2 describes the research methods, including performance indicator simulation programs, generative design parameter settings, and data analysis and visualization techniques. Section 3 presents the research results, focusing on the exploration of the multi-objective optimization process and the various form outcomes generated by generative design. Section 4 discusses the results and the potential for performance improvement through optimization, as well as the limitations of the study. Section 5 provides conclusions and future outlook.

2. Methodology

This study combines generative design and multi-objective optimization methods to create a design workflow, focusing on optimization directions such as outdoor thermal comfort and building energy consumption, as shown in Figure 1. The research spans three stages, from subjective perception to performance improvement in the built environment: (1) perception detection; (2) analysis, diagnosis, and management; (3) quality efficiency improvement. Furthermore, the research involves five specific steps: (1) subjective perception; (2) urban modeling; (3) building performance simulation; (4) block scale building form generation; and (5) multi-objective genetic optimization.

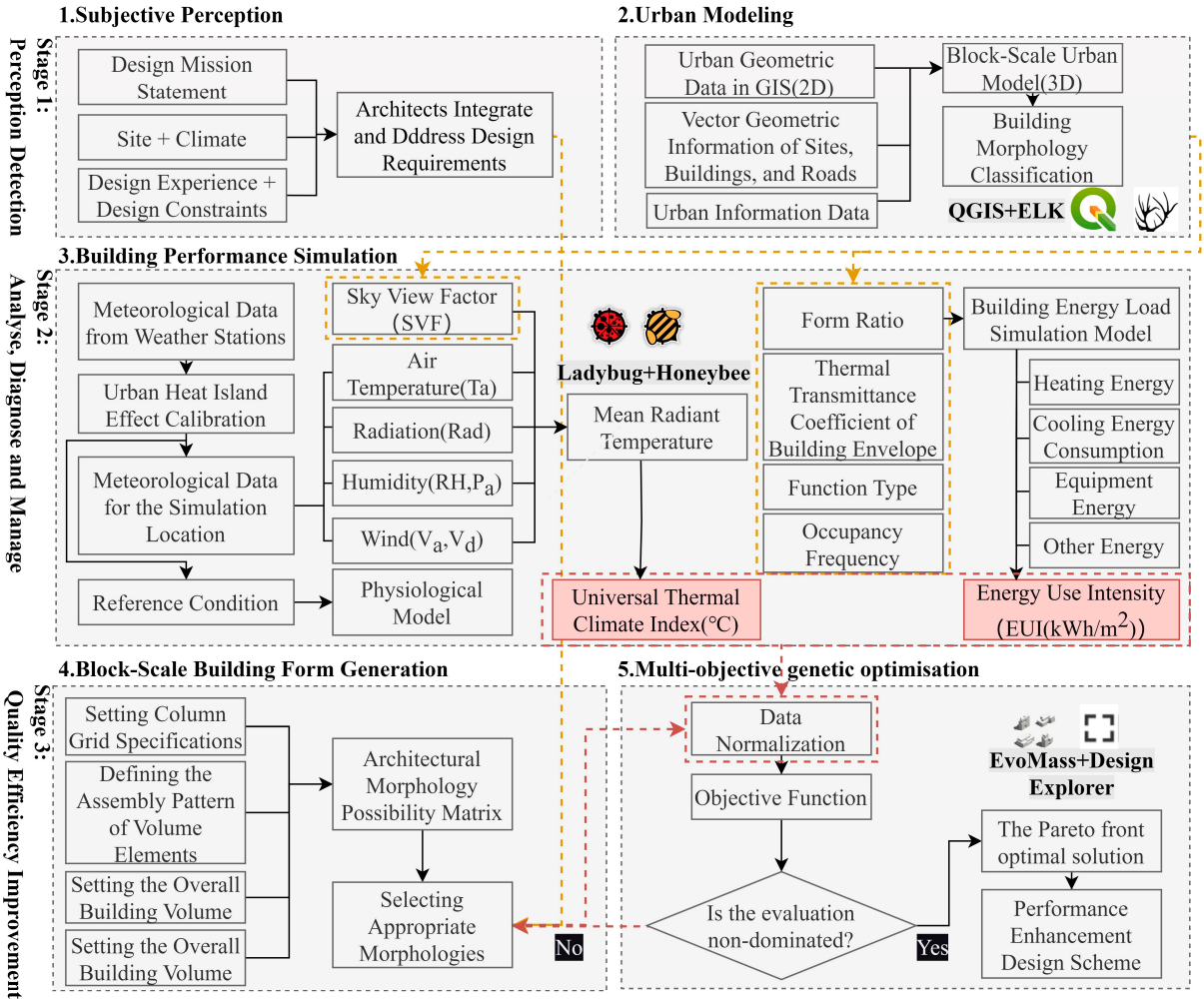

Figure 1. Technology roadmap.

In the morphological generation process, parameters such as enclosure ratio, building height, floor area, floor area ratio, and orientation offset angle are selected. Rhino and EvoMass are used as modeling and parametric form generation platforms, while Ladybug Tools serves as the performance simulation platform, simulating outdoor thermal comfort and annual building energy consumption [22,23]. The Universal Thermal Climate Index (UTCI) is used as the performance metric for outdoor thermal comfort, supplemented by secondary indicators such as Predicted Mean Vote (PMV), Mean Radiant Temperature (TMRT), Sky View Factor (SVF), and Air Temperature (Ta). Energy Use Intensity (EUI) is used as the performance metric for building energy consumption, with sub-metrics including heating energy consumption (Heat Generation), air conditioning and refrigeration (Chiller), lighting energy consumption (Lighting), other electrical equipment (Equipment), and total energy

load (Total Load) [24,25]. Using the generative design program [26–28], multiple form indicators are selected as optimization targets, iterating and optimizing within a multi-objective optimization cycle.

2.1. Research Location

Dalian (latitude 38.91° N, longitude 121.61° E) is a major city and sub-provincial municipality in China, with a permanent population of 7.539 million and a total area of 12,574 km^2. Located at the southernmost point of northeast China, Dalian consists of 10 districts and counties, including Zhongshan District, Shahekou District, Xigang District, Ganjingzi District, Pulandian District, Changhai County, Jinzhou District, Zhuanghe City, Wafangdian City, and Lushunkou District. The city has a temperate monsoonal climate with maritime characteristics, featuring mild winters and warm summers with distinct seasons. The average annual temperature is 10.5 °C, with annual precipitation ranging between 550 and 950 mm and total annual sunshine duration between 2500 and 2800 h. In recent years, the occurrence of extreme weather events in China has increased [29], with both summer heatwaves and harsh winter cold significantly impacting urban thermal perception, inevitably increasing the use of air conditioning, heating, and other electrical equipment.

The study site is located in the Huaxin Industrial Park, Ganjingzi District, Dalian, as shown in Figure 2. The designated plot spans 126,000 m^2. The existing building on-site is an L-shaped office building with built structures on the south and east sides and open spaces to the north and west. An urban road on the south side connects the site with its surroundings. To the southwest and north of the site are office and residential buildings, respectively, arranged as linear standalone blocks. A digital model of the existing buildings and site conditions was created using the Grasshopper-Elk urban modeling workflow. This model was integrated with a multi-objective optimization design method to optimize the form of office buildings within the site.

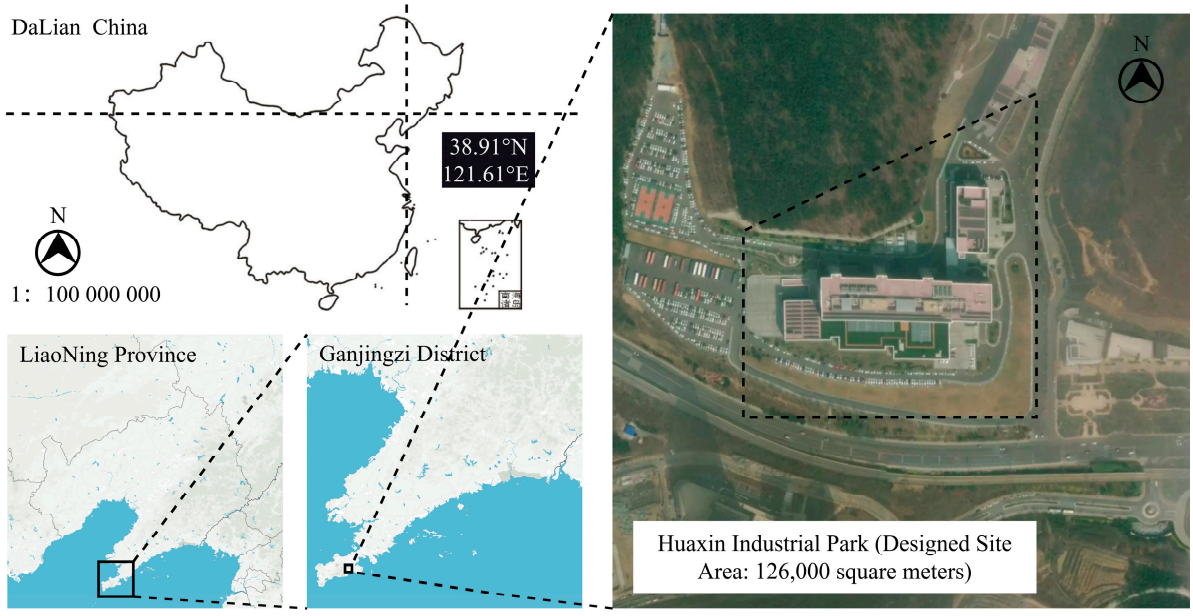

Figure 2. Research site location and existing building satellite map. Note: The base map is a standard map, and there are no modifications to the map. The map review number is GS (2016) 1552.

This section offers context regarding the research location, climate, and site-specific characteristics, emphasizing the practical challenges faced by the design process. The detailed modeling workflow, combining urban-scale modeling with form optimization,

provides a foundation for generating adaptive and high-performance design solutions tailored to Dalian's climate and urban environment.

2.2. Energy Load Simulation

In its broad definition, building energy consumption refers to the total energy used throughout the entire life cycle of a building, including the production and transportation of building materials, the construction phase, the operational phase, and the demolition phase. In a narrower sense, building energy consumption specifically refers to the energy used during the operational phase, encompassing heating and air conditioning, lighting, and equipment energy use. The primary energy sources include water, electricity, natural gas, coal, and biomass. This study focuses on passive design strategies, which are significantly influenced by building morphology [30] and are directly controlled by architects. Active systems, such as heating, ventilation, and air conditioning (HVAC) system design [31], are beyond the scope of this research. The building energy consumption simulation only considers the operational phase [32,33], excluding the energy required for construction and demolition.

To simplify the building energy simulation calculations [34–36], the building envelope is modeled as a zero-thickness plane with a certain thermal resistance. This approach aligns with the guidelines outlined in the "General Specification for Building Energy Efficiency and Renewable Energy Utilization (GB55015-2021 [37])" for the cold A and B zones in China. The thermal transmittance of the building envelope has a significant impact on heating energy consumption, as heat loss due to the temperature difference between indoor and outdoor spaces during the heating season is dominant. The window-to-wall ratios for south-, north-, east-, and west-facing walls are set at 0.55, 0.35, and 0.40, respectively. The thermal transmittance values for external walls, roofs, and floors are set to 0.35 $W/m^2 \cdot K$, 0.25 $W/m^2 \cdot K$, and 0.35 $W/m^2 \cdot K$, respectively, with heating energy consumption for cold regions calculated at 82 $MJ/(m^2 \cdot a)$. The hourly occupancy rates are shown in Table 1.

Table 1. Room occupancy rates (in percent).

Building Type		Time											
		1	**2**	**3**	**4**	**5**	**6**	**7**	**8**	**9**	**10**	**11**	**12**
Office Building	Weekdays	0	0	0	0	0	0	10	50	95	95	95	80
	Holidays	0	0	0	0	0	0	0	0	0	0	0	0
		13	14	15	16	17	18	19	20	21	22	23	24
	Weekdays	80	95	95	95	95	30	30	0	0	0	0	0
	Holidays	0	0	0	0	0	0	0	0	0	0	0	0

The building energy consumption simulation utilizes the Honeybee 0.0.69 plugin from Ladybug Tools 1.6.0, which allows Rhino 7.0 models to be imported into EnergyPlus 9.5.0 and OpenStudio 3.4.0 for energy analysis. The steps for the building energy simulation experiment are as follows. (1) Model validation: Import the model into Grasshopper 2.0 to check for and eliminate any overlapping surfaces. Once the model is verified, import it into Honeybee, assigning material properties to components such as external walls, roofs, and floors based on predefined parameters. (2) Setting basic parameters: Define the schedule based on the functional zoning requirements and input the local climate data for Dalian, provided by the national meteorological service. (3) Building the energy model: Construct the Building Energy Model (BEM) within Honeybee. The model primarily consists of HB Room and Context, where HB Room includes elements such as HB Object, Construction Set, Program, and Conditioned space definitions. (4) Generating energy simulation results:

Simulate to output annual Energy Use Intensity (EUI), heating energy consumption, and cooling energy consumption. The energy use is calculated in units of kWh/m^2. (5) Visualization of simulation results: Organize the energy consumption data, make necessary adjustments, and use Origin software 2023 to visualize the experimental results.

2.3. Outdoor Thermal Comfort Simulation

Thermal comfort, also known as thermal satisfaction or thermal comfort level, refers to the human body's feedback on the comfort level of the thermal environment [38]. Research on thermal comfort initially began in the fields of indoor environmental design and heating, ventilation, and air conditioning (HVAC), later expanding to outdoor spaces in landscape architecture, specifically referred to as outdoor thermal comfort. Comfort is defined as the degree of satisfaction individuals feel, both physiologically and psychologically, with the objective physical environment, which includes factors such as thermal conditions, lighting, acoustics, and air quality [39]. When subjective evaluations are involved, other factors like cognition, psychology, and personal habits must also be considered [40,41].

Thermal comfort describes a state where individuals feel satisfied with the thermal conditions of their surroundings, which is influenced by factors such as air temperature, humidity, wind speed, and solar radiation. In this study, the term "comfort" specifically refers to thermal comfort, one of the earliest research topics in the field of building science. Thermal comfort is affected by multiple factors, including environmental conditions, human factors, and climatic influences.

Simulations of outdoor thermal comfort and building energy consumption were performed using the Rhino-Grasshopper platform [42–44], incorporating plugins such as Ladybug, Dragonfly, and Honeybee [45]. The thermal environment simulation results are quantified through several indices, including the Universal Thermal Climate Index (UTCI), Predicted Mean Vote (PMV), and Mean Radiant Temperature (TMRT). The research process follows these key steps. (1) Sky View Factor (SVF) Simulation: The Sky View Factor (SVF) simulates the extent to which a person is exposed to the sky, used to assess the natural impact of sunlight on individuals in outdoor environments. In building design, evaluating SVF is a crucial parameter for assessing building morphology. This index is calculated by considering factors such as building orientation, height, and angle. The input is defined through "LB Human to Sky Relation", which sets the measurement points and site locations, while the output is generated by "LB Outdoor Solar TMRT", which calculates solar irradiance under shadow conditions in outdoor environments. (2) Mean Radiant Temperature (TMRT) Simulation: Mean Radiant Temperature (TMRT), also referred to as ambient or environmental temperature, is the temperature at which the total radiant energy emitted by all surrounding surfaces is uniformly distributed at a given time. TMRT is crucial for describing the overall thermal radiation environment surrounding an individual. Although it represents an idealized temperature value, TMRT plays a significant role in both human thermal comfort and building energy consumption. During winter, people typically adjust indoor temperatures to maintain comfort, and the level of TMRT can influence heat loss and retention. In summer, elevated TMRT values can increase building energy consumption, as higher radiant temperatures require more cooling energy from air conditioning systems to maintain comfortable indoor conditions.

$$T_{mrt} = \left[\left(T_g + 273 \right)^4 + \frac{1.10 \times 10^8 V_a^{0.6}}{\varepsilon D^{0.4}} \left(T_g - T_a \right) \right]^{\frac{1}{4}} - 273 \quad (1)$$

The "LB Outdoor Solar TMRT" program in the Ladybug software 0.0.69 utilizes the "Solar Cal" model from ASHRAE-55 [46] to calculate both long-wave and short-wave solar radiation. This model estimates the Mean Radiant Temperature (TMRT) using the

sky view factor. The output provides hourly simulated values of TMRT. In addition to these calculations, the simulation can be refined by incorporating parameters such as human activity level, clothing insulation, metabolic rate, and ground surface reflectivity, as shown in Formula (1). (3) Outdoor Thermal Comfort Simulation: The Universal Thermal Climate Index (UTCI) is a metric that evaluates and describes human comfort based on physiological and psychological responses to the thermal environment. Influencing factors include temperature, humidity, airflow speed, and radiant temperature, along with the body's physiological and psychological reactions to these environmental conditions. The UTCI assumes a walking activity with a metabolic rate of 2.4 met, and it automatically adjusts clothing insulation based on outdoor temperatures. Although originally designed for indoor environments, the UTCI provides architects with a quantifiable method to analyze user comfort, allowing them to design and modify environments to improve overall comfort and health.

The UTCI has several advantages. (1) It is applicable under various thermal exchange conditions; (2) it can be used across a wide range of climates, seasons, and scales; (3) it supports interdisciplinary research across fields such as meteorology, geography, and architecture, as shown in Formula (2).

$$UTCI = T_a + offset(T_a, T_{mrt}, V_a, RH) \quad (2)$$

The "LB UTCI Comfort" module for UTCI calculation takes four key climate parameters as inputs: air temperature, mean radiant temperature, relative humidity, and wind speed. The output generates a thermal map of the simulated site, displaying hourly UTCI values and the corresponding outdoor thermal comfort zones. This process allows for the selection of grid points within the site as simulation points for multiple UTCI calculations, with the results visualized to depict the distribution of outdoor thermal comfort across the site.

2.4. Standardization Processing and Objective Function

Building energy consumption and outdoor thermal comfort are two performance indices with different dimensions, making them challenging to optimize as single-objective problems through direct target function settings [47]. This necessitates data preprocessing [48]. In this study, dimensionless data processing is employed, as demonstrated in Formula (3). In this equation, the greater the difference between a performance index value and its maximum, the smaller the resulting standardized value. The standardized value indicates the relative magnitude of a specific value within the total range of values, which lies between 0 and 1. For building energy consumption, the objective function is to minimize the total building energy consumption. For outdoor thermal comfort, the neutral thermal temperature serves as the reference point, comparing individual values to this neutral temperature. The objective function aims to minimize the deviation from the neutral temperature, thus making the simulated site temperatures as close as possible to the neutral thermal zone.

$$x_i' = \frac{maxx_i - x_i}{maxx_i} \quad (3)$$

The designated objective function needs to articulate a formulaic expression that simultaneously optimizes for both comfort and energy consumption. Through the normalization of indices, it is possible to balance two types of data that differ in units and have significant numerical disparities. The traditional method of balancing uses Formula (4), which employs a balancing factor w to weigh the two performance indices. For instance, if the weight for building energy consumption is set at w = 0.6, then the balancing factor for thermal comfort should be 0.4. However, this method is susceptible to subjectivity in

setting the weight factors, potentially leading to suboptimal results constrained by personal biases, often resulting in a locally optimal solution (LOS). In this study, the weight factor w is set to 0.5.

This research adopts the Pareto optimization approach to enhance solution finding, effectively avoiding local optima. The core of Pareto optimization lies in identifying the optimal frontier. Points on this frontier are Pareto optimal solutions. If a testing scheme's two-dimensional performance scatter plot shows no dominated solutions, the scheme is considered a Pareto optimal solution. All such optimal solutions form a scattered set, which, when connected, creates the Pareto frontier. This method minimizes subjective interference in the optimization process. The criteria for forming a Pareto optimal solution involve setting objective functions to simultaneously minimize both indices—building energy consumption and thermal comfort—as shown in Formula (5). Performance indices are evaluated using a fitness metric, which represents the normalized result of the performance simulation.

The designated objective function needs to articulate a formulaic expression that simultaneously optimizes for both comfort and energy consumption. Through the normalization of indices, it is possible to balance two types of data that differ in units and have significant numerical disparities. The traditional method of performance simulation.

$$minize\ Total\ Fitness = wFitness\ of\ Load + (1 - w)Fitness\ of\ Comfort \tag{4}$$

$$minize(Total\ Fitness) = minize\begin{pmatrix} Fitness\ of\ Load \\ Fitness\ of\ Comfort \end{pmatrix} \tag{5}$$

2.5. Multi-Objective Optimization

In practical design engineering projects, the challenge often lies in simultaneously coordinating multiple project objectives. Architectural performance goals such as thermal comfort and energy consumption require differing approaches to building form, and historically, balancing these objectives has heavily depended on the experience and intuition of architects. However, with the advancement of quantitative science, multi-objective optimization methods have emerged to address the deficiencies in coordinating multiple building performance indices. The non-dominated set of solutions in multi-objective optimization is considered as Pareto optimal solutions, with the optimization direction aimed at minimizing each objective, thus optimizing multiple objectives $F(x)$ simultaneously. The formula is as follows:

$$\begin{array}{ll} minimize & F(x) = (f_1(x),\ f_2(x),\ \ldots,\ f_m(x))^T \\ subject\ to & x \in \Omega \end{array} \tag{6}$$

According to Formula (6), each $F_i(x)$ represents an individual objective function associated with different performance criteria of the building project. This approach facilitates a systematic exploration of architectural solutions, enabling the integration of multiple performance metrics without undue compromise. The adoption of multi-objective optimization allows architects and engineers to derive balanced solutions that better meet the complex demands of modern building projects.

Outdoor thermal comfort and building energy consumption are critical determinants of architectural form variations, with the thermal comfort index subdivided into several metrics such as Sky View Factor (SVF), Mean Radiant Temperature (MRT), Universal Thermal Climate Index (UTCI), and Predicted Mean Vote (PMV), denoted as Index1, Index2, Index3, Index4, respectively. Moreover, the building layout is influenced by foundational architectural parameters, with adjustable building parameters, including Width, Length,

Orientation, and Capacity Ratio. In this setting, architectural form parameters serve as independent variables, which are freely generated through the EvoMass system based on morphological parameters [49]. Performance parameters are treated as dependent variables for evaluating generated designs [50].

Architectural volume generation is facilitated through the Additive Form Massing Component, based on a summary of morphological parameters for office buildings in Dalian, as discussed in Chapter 4. Key morphological settings include an 8×8 column grid system with 8 m spacing, building heights ranging from 6 to 10 stories, and a floor height of 4 m. Additionally, building orientation uses true south as a reference, with a variation angle range from -15° to 15° and a granularity of 1°.

For optimizing outdoor thermal comfort, the annual average UTCI value is used as a quantitative index to ensure that the site surrounding the building volume remains as close to thermal neutrality as possible. For energy consumption optimization, the energy load per unit area serves as a quantitative index, with initial energy consumption parameters set to simulate the annual energy consumption of the building form. To balance these performance goals, the research employs the Pareto optimal solution method to weigh the importance of multiple design objectives, optimizing them simultaneously. To simplify calculations, the UTCI simulation resolution is set at 50 m $\times$ 50 m, with averages from each generated site scenario used as quantitative metrics.

The optimization design process is implemented through the Steady State Island Evolutionary Algorithm, with five islands optimizing concurrently, each containing 15 individuals. A total of 1400 optimization iterations are conducted to ensure adequate evolution.

3. Results

3.1. Multi-Objective Optimization Result Analysis

Figure 3 illustrates the distribution of all generated samples, with the horizontal and vertical axes representing the standardized values of outdoor thermal comfort and building energy consumption, respectively. The overall trend in the optimization scatterplot shows the samples converging toward the minimal values of the two performance indices [51], indicating that the multi-objective optimization method successfully addresses the aim of balancing multiple performance indices [52,53]. Additionally, most optimized design samples exhibit performance indicators superior to existing buildings. However, since actual design processes involve multiple factors, there are numerous other influences to consider beyond just outdoor thermal comfort and building energy consumption.

Significantly, building orientation has a notable impact on performance-based design. From the solutions on the Pareto frontier, it is evident that south or southeast orientations are optimal. A south-facing orientation allows more direct sunlight during the day, reducing the need for artificial lighting and thereby lowering energy consumption. Conversely, buildings facing southeast create more shadows over the courtyard, maintaining more of the site in a thermally neutral comfort zone, thus improving the thermal environment.

A total of 1500 multi-objective optimization schemes were generated, with the distribution of optimization samples from six islands, as shown in Figure 3. The figure combines the individual and aggregate relationships. The y-axis represents the standardized result of outdoor thermal comfort, while the x-axis represents the standardized total annual building energy consumption. The black line represents the Pareto frontier's optimal solutions, indicating the best outcomes in the optimization direction. The objective of the optimization design is to minimize the standardized indices, with points closer to the origin representing better outcomes. Since multiple islands can produce multiple optimal solutions, the research consoli-

dates these island-specific optima into an optimal solution set, providing design tendencies and optimization suggestions for the early stages of architectural form design [54].

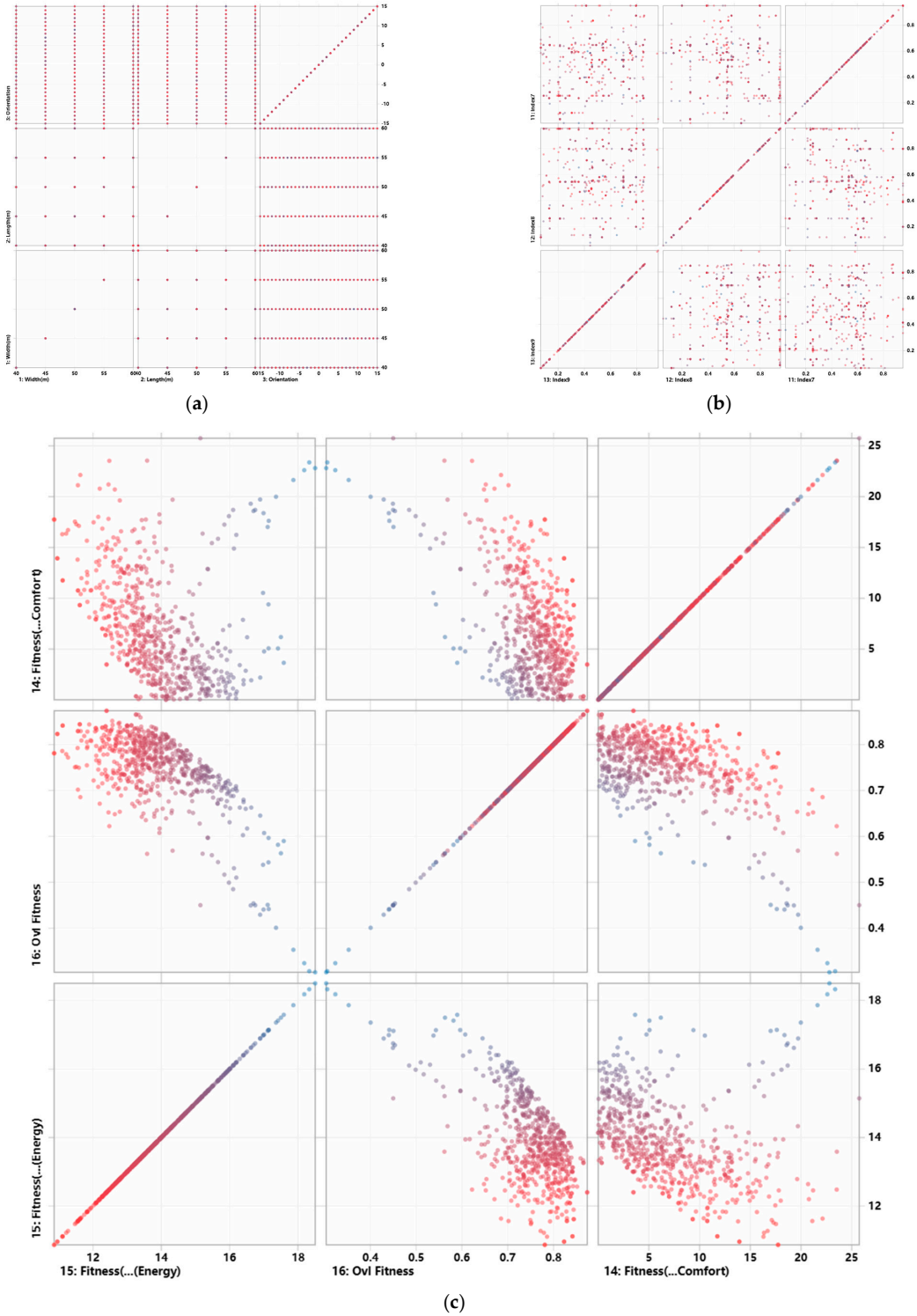

(**a**) (**b**) (**c**)

Figure 3. Distribution of optimal solutions for the optimized sample. (**a**) Performance Distribution of the Pre-Iteration Design; (**b**) Performance Distribution of Design Solutions during Iteration; (**c**) Post-Iteration Design Distribution.

The performance of the optimal solutions generated after multi-objective optimization is shown in Figure 3. The axes represent a combination of the fitness of energy consumption (Fitness of Energy), thermal comfort fitness (Fitness of Comfort), and overall

fitness (Total Fitness). The dense clustering of points around the origin in the energy consumption–thermal comfort graph indicates that, under the multi-objective orientation, the iteratively generated schemes approach the performance envisioned by the objective function. The interaction of these indices is not merely additive but involves iterative optimization coordinated through the control of morphological parameters. The degree of clustering observed in the graph signifies the efficacy of multi-objective optimization, with performance enhancements realized during the iterative process.

Figure 3 depicts the iterative process of multi-objective optimization for a selected set of 650 solutions. In the initial settings of optimization, the individual geometric parameters of the building are set uniformly across gradients, as evidenced by the uniform intersection of lines in the early segments of the line graph. During the mid-stage of optimization, after evaluating multiple performance indices, a comprehensive assessment of the solutions' performance across several dimensions is conducted. Non-dominant solutions are replaced by dominant ones. In the later stages of optimization, as the number of iterations increases, the overall trend lines show a clustering tendency, and the optimal solution set on the Pareto front outperforms other non-dominated solution sets, ultimately outputting the Pareto optimal solutions.

Figure 4 illustrates the performance optimization process for 12 selected Pareto optimal solutions. The continuous lines from left to right represent each specific scheme, and the vertical axis marks indicate the standardized values of that performance standard. The distribution of fitness levels among the optimal solutions indicates that each solution exhibits distinct performance characteristics. Some schemes emphasize indices related to outdoor thermal comfort, while others focus on building energy consumption, yet all display excellent overall fitness. Thus, the multi-objective optimization not only coordinates various building performance goals but also highlights distinctive features compared to other optimal solutions.

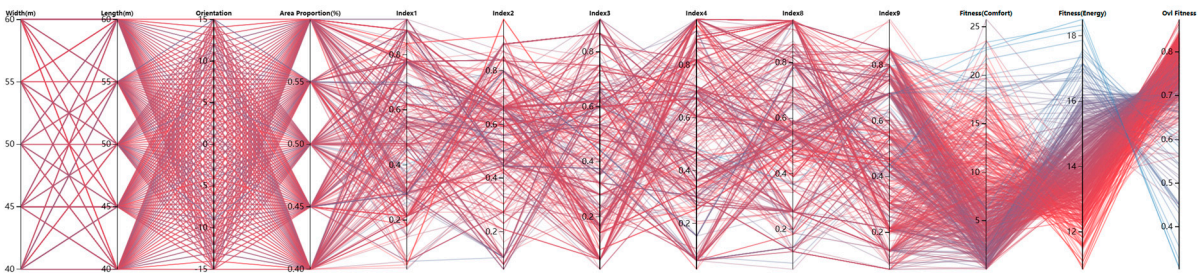

(**a**)

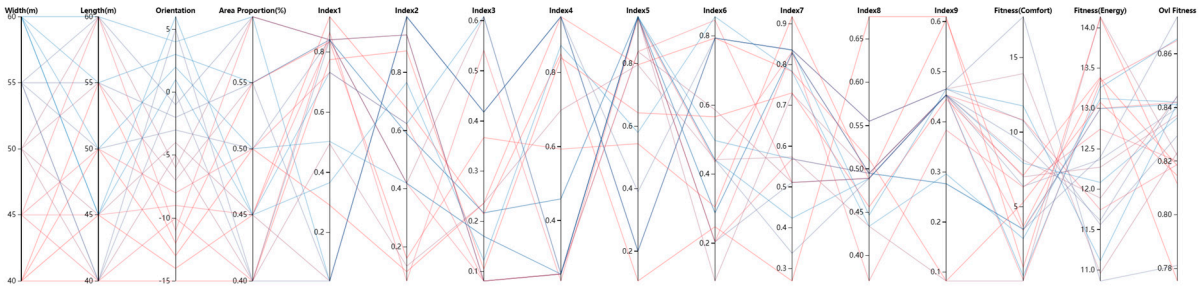

(**b**)

Figure 4. Pareto Chart of Optimal Solutions. (**a**) Pareto Front of the Entire Solution Set; (**b**) Pareto Front of the Optimal Solutions.

Table 2 delineates the iterative process of multi-objective optimization across a set of 650 optimal solutions. Initially, individual geometric parameters of the buildings are

uniformly set across gradients, as illustrated by the uniform crossing of lines in the early segment of the line graph. During the mid-phase of optimization, after evaluating various performance indices, solutions are comprehensively assessed across multiple dimensions. Non-dominant solutions are replaced by dominant ones. In the later stages, as the number of iterations increases, the trend lines converge, indicating clustering. The optimal solution set on the Pareto front (Pareto frontier) exhibits superior performance relative to other non-dominated solution sets, culminating in the selection of the Pareto optimal solutions.

Table 2. Multi-objective optimization process.

Optimization Results from Iteration 0 to Iteration 10		
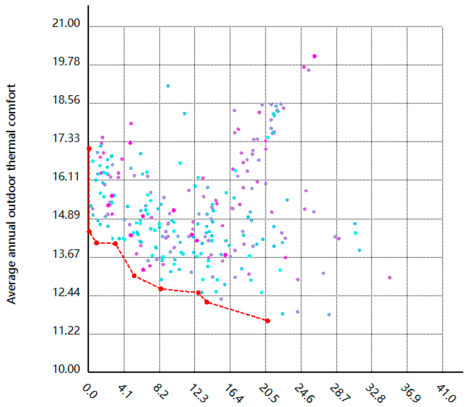 Current Mutation Rate: 0.3119 Current Mutation Radius: 0.9085	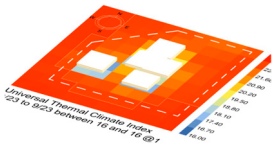 ID: 64 Fitness of load: 16.98 Fitness of comfort: 13.03	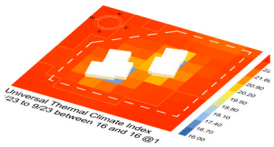 ID: 128 Fitness of load: 1.03 Fitness of comfort: 16.99
	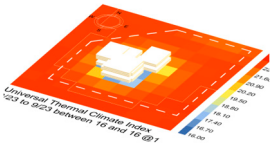 ID: 192 Fitness of load: 1.38 Fitness of comfort: 14.70	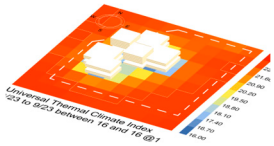 ID: 256 Fitness of load: 6.74 Fitness of comfort: 16.37
Optimization Results from Iteration 10 to Iteration 20		
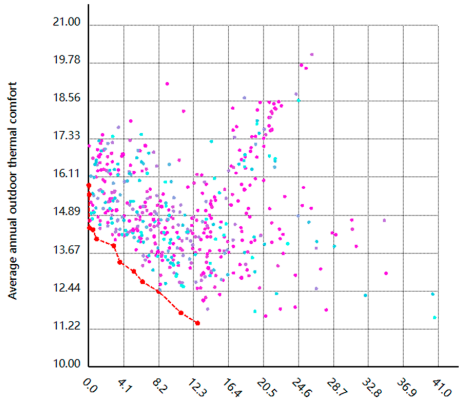 Current Mutation Rate: 0.2695 Current Mutation Radius: 0.8068	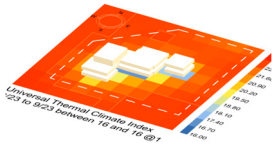 ID: 320 Fitness of load: 17.09 Fitness of comfort: 17.39	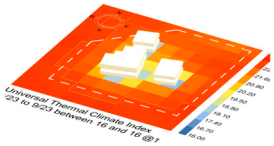 ID: 384 Fitness of load: 0.84 Fitness of comfort: 15.11
	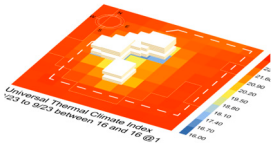 ID: 448 Fitness of load: 19.39 Fitness of comfort: 14.18	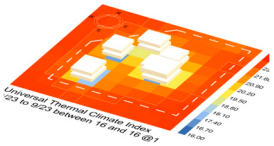 ID: 512 Fitness of load: 7.58 Fitness of comfort: 14.74
Optimization Results from Iteration 40 to Iteration 50		
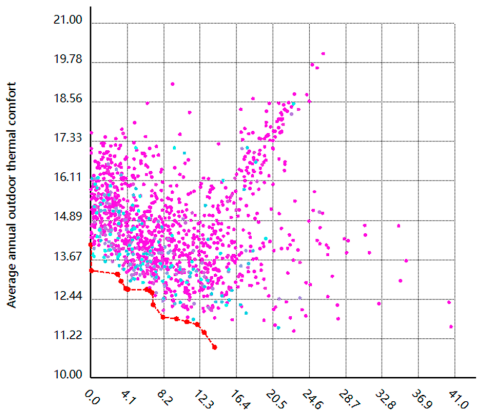 Current Mutation Rate: 0.1424 Current Mutation Radius: 0.5017	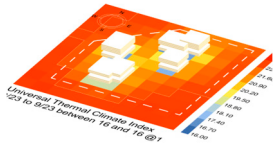 ID: 1088 Fitness of load: 1.79 Fitness of comfort: 15.43	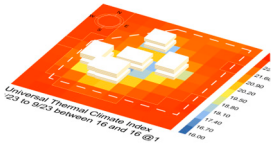 ID: 1152 Fitness of load: 4.79 Fitness of comfort: 15.67
	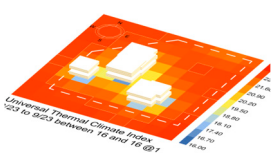 ID: 1216 Fitness of load: 1.59 Fitness of comfort: 13.62	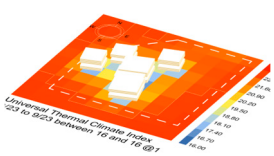 ID: 1280 Fitness of load: 2.89 Fitness of comfort: 15.60

Table 2. *Cont.*

Optimization Results from Iteration 50 to Iteration 60		
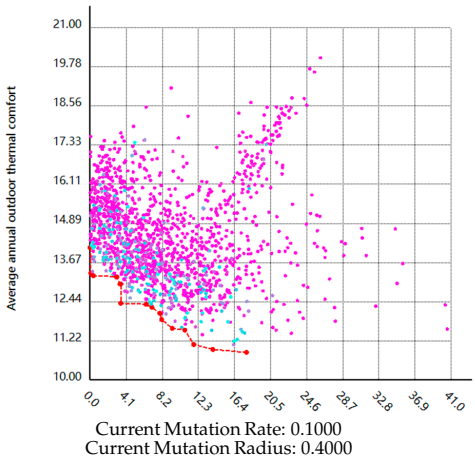 Current Mutation Rate: 0.1000 Current Mutation Radius: 0.4000	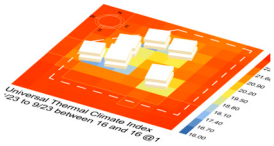 ID: 1344 Fitness of load: 8.41 Fitness of comfort: 14.90	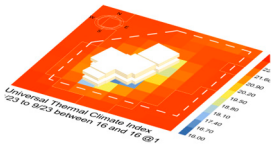 ID: 1408 Fitness of load: 13.80 Fitness of comfort: 11.54
	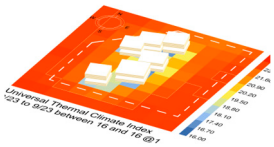 ID: 1472 Fitness of load: 3.84 Fitness of comfort: 14.01	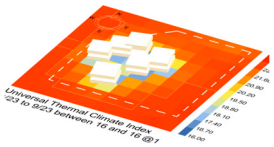 ID: 1536 Fitness of load: 1.82 Fitness of comfort: 14.12

Figure 4a,b depict the performance optimization process for 12 Pareto optimal solutions with distinct morphological features. The continuous lines from left to right in each figure represent individual schemes, with the vertical axes indicating the standardized values of the performance standards. The fitness distribution of the optimal solutions reveals significant differences in performance, with each scheme exhibiting distinct characteristics. Some schemes prioritize indices related to outdoor thermal comfort, while others focus on reducing building energy consumption, yet all demonstrate exceptional overall fitness. Therefore, the multi-objective optimization not only reconciles multiple building performance objectives but also distinguishes the optimal solutions in terms of their distinct characteristics compared to other potential solutions.

3.2. Comparison of Performance Before and After Optimization

Figure 5a,b illustrate the distribution of the Universal Thermal Climate Index (UTCI) and Predicted Mean Vote (PMV) before optimization. The original design scenario indicates an annual average daytime UTCI ranging from 22.89 °C to 27.84 °C within a 500 m × 500 m site, with an area-wide average UTCI of 10.10 °C. The minimum UTCI values are located at the northern L-shaped corner of the building. The PMV simulation identifies thermal sensations as follows: warm sensations constitute 20.04%, neutral sensations 34.69%, and cool sensations 45.26%. The zones classified as thermally neutral are concentrated around the building block but cover a small area, located 3–5 m from the building boundary and accounting for 34.69% of the total site.

Figure 5c,d present the UTCI and PMV distributions following the optimization process. Post-optimization, the UTCI values range from 9.11 °C to 10.46 °C during average daytime, with a site average UTCI of 9.79 °C. According to the UTCI thermal comfort scale, the average conditions are categorized as experiencing 'no thermal stress', showing no significant change in average UTCI compared to the original design. However, the area of thermal comfort has increased significantly from approximately 60% of the site in the original design to about 75% in the optimized design. This expansion indicates an improvement in the UTCI performance index. The PMV distribution after optimization shows thermal sensations divided as follows: warm sensations at 18.37%, neutral at 35.80%, and cool at 45.86%. The proportion of thermally neutral sensations has improved by 1.11% compared to the original scenario.

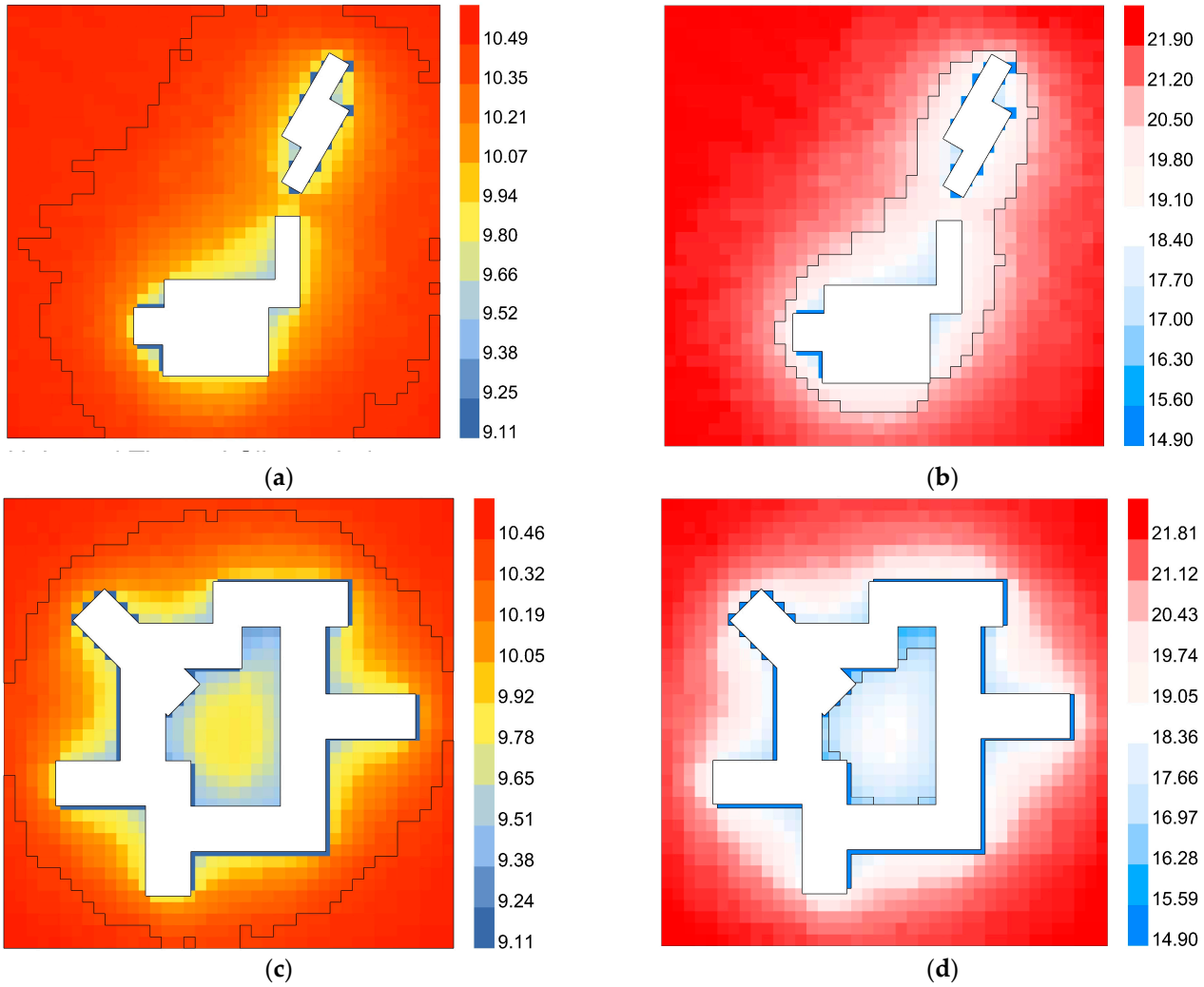

Figure 5. Distribution maps of UTCI and PMV before and after optimization. (**a**) The thermal comfort distribution heatmap before optimization: Average UTCI: 10.10 °C; (**b**) The thermal sensation vote distribution heatmap before optimization: Percentage of hot sensation: 20.04%, percentage of neutral sensation: 34.69%, percentage of cold sensation: 45.26%; (**c**) Thermal comfort distribution heatmap after optimization: Average UTCI: 9.79 °C; (**d**) The thermal sensation vote distribution heatmap after optimization: Percentage of hot sensation: 18.37%, percentage of neutral sensation: 35.80%, percentage of cold sensation: 45.86%.

The optimization of the design has enhanced thermal environment performance indicators significantly over the original scenario. The increase in the area classified as 'no thermal stress' and the improvement in the proportion of thermal neutrality highlight the effectiveness of the optimization in increasing occupant comfort and the efficient use of space with respect to thermal indices.

Table 3 presents the pre-optimization monthly building energy consumption data. According to the simulation, the total energy consumption of the original design was 75.68 kWh/m^2 per year. This included 44.43 Wh/m^2 for cooling, 1.91 Wh/m^2 for heating, 31.14 Wh/m^2 for lighting, and 31.19 Wh/m^2 for equipment usage. Table 3 illustrates the post-optimization energy consumption, where the total decreased to 62.88 kWh/m^2 per year. The breakdown is as follows: cooling energy consumption significantly reduced to 8.79 Wh/m^2, heating remained nearly unchanged at 1.87 Wh/m^2, lighting was reduced to 21.31 Wh/m^2, and equipment energy slightly increased to 31.91 Wh/m^2.

Table 3. Data Sheet of Building Energy Consumption before and after Optimization.

	January	February	March	April	May	June	July	August	September	October	November	December
Optimized Plan—Cooling	0.00	0.00	0.00	0.00	0.03	0.94	3.36	3.11	1.23	0.12	0.00	0.00
Optimized Plan—Heating	0.77	0.37	0.15	0.02	0.00	0.00	0.00	0.00	0.00	0.00	0.07	0.49
Optimized Plan—Lighting	1.80	1.64	1.87	1.67	1.87	1.79	1.74	1.87	1.74	1.80	1.79	1.74
Optimized Plan—Equipment	2.62	2.37	2.67	2.48	2.67	2.57	2.58	2.67	2.53	2.62	2.57	2.58
Original Plan—Cooling	0.00	0.00	0.00	0.00	0.03	1.18	4.45	4.12	1.53	0.13	0.00	0.00
Original Plan—Heating	0.78	0.38	0.15	0.02	0.00	0.00	0.00	0.00	0.00	0.00	0.07	0.49
Original Plan—Lighting	2.62	2.38	2.71	2.50	2.71	2.58	2.58	2.68	2.58	2.63	2.61	2.58
Original Plan—Equipment	2.67	2.37	2.68	2.52	2.69	2.61	2.59	2.67	2.54	2.67	2.58	2.62

Both schemes show similar trends in energy consumption, particularly for lighting and equipment usage, which remain consistent throughout the months, ranging between 2.4 Wh/m^2 and 2.7 Wh/m^2 for equipment and 1.6 Wh/m^2 to 1.9 Wh/m^2 for lighting. Heating energy consumption shows values from May to October, coinciding with the cooling months set according to meteorological data. Notably, the optimized design significantly reduces cooling energy consumption, especially in July and August, by approximately 1.1 Wh/m^2. This reduction is attributed to the more complex building massing in the optimized design, which creates self-shading effects that lower indoor temperatures and reduce cooling needs during summer.

Table 3 illustrates the monthly total energy consumption and energy-saving efficiency of the original and optimized schemes. The dual y-axis graph displays total energy consumption on the left and energy-saving efficiency on the right. Bar charts represent energy consumption, and line graphs depict the differences and percentage changes in energy consumption pre- and post-optimization. For instance, the original scheme consumed 6.07 Wh/m^2 in January, while the optimized scheme used 5.19 Wh/m^2, achieving an energy-saving efficiency of 14.49%. The yearly energy-saving efficiency ranges from 14.49% in January to 20.16% in July, with an average of 16.66%. The highest savings in July likely result from the self-shading provided by the optimized architectural form, which is most effective during summer, as seen in the seasonal analysis: Summer > Autumn $\geq$ Spring > Winter.

This analysis demonstrates that the multi-objective optimization set for architectural design enhances performance significantly over the original scheme, particularly in reducing energy consumption during peak cooling periods.

4. Discussion

The Pareto optimal solutions, compared with existing approaches, can significantly improve the UTCI while simultaneously reducing the EUI level. The fitness of a solution reflects its specific performance in a certain aspect. Since the optimization trend minimizes the fitness of two performance indicators, the set of solutions distributed along the Pareto front demonstrates better overall performance. The set of Pareto optimal solutions is shown in Figure 6, where the range of the sum of the fitness for outdoor thermal comfort and building energy consumption across the 16 optimal solutions is between 13.40 and 30.74. Among them, the solution with the smallest total fitness sum is ID 1444, which has an energy consumption fitness (Fitness of load) of 3.48 and an outdoor thermal comfort fitness (Fitness of comfort) of 12.99. This solution features multiple building blocks that form an enclosed central courtyard located on the east side. It can be observed that buildings with a higher enclosure degree are more adaptable to cold climates, demonstrating stronger performance in both outdoor thermal comfort and energy consumption.

However, there are still limitations in this study. (1) The HVAC system performance was simplified in the simulation process, and the simulation method has not been validated, which resulted in significant deviations in the energy consumption simulation values. (2) The weight setting for energy consumption and thermal comfort was set to w = 0.5, but in practical design, the weight coefficients for each performance aspect should be dynamically adjusted based on real-world conditions and design requirements. (3) In reality, the building

design process is complex, and building forms are often the result of a combination of factors such as ideology, cultural spirit, and economic conditions. However, due to the current limitations of simulation hardware and computational power, multi-objective optimization cannot incorporate as many influencing factors into the objective functions as desired, leading to discrepancies with real-world situations. (4) The core algorithm for multi-objective optimization has been updated to NSGA-III, which has improved optimization efficiency and results compared to NSGA-II. However, this study did not use the latest multi-objective optimization technology for optimization.

Figure 6. Pareto Front Solutions of Building Forms.

5. Conclusions

Computational generative design is an important topic in the context of the era of performance enhancement. This study demonstrates the significant potential of multi-objective optimization and generative design in architectural design. The Pareto optimal solutions coordinate two primary optimization goals: "reducing building energy load" and "improving outdoor thermal comfort for occupants". These solutions can be applied to the early-stage massing design and measurement of office buildings under a green and health-oriented design approach. The results show that: (1) forms with higher enclosures (three-sided or four-sided) are more suitable for office buildings in cold regions in terms of both outdoor thermal comfort and building energy consumption; (2) compared with

existing building designs, the Pareto optimal solution improves energy efficiency by 16.55% over the course of the year under 2022 meteorological conditions, and the proportion of outdoor thermal neutrality increases by 1.11%. The results indicate that the optimized design can balance building energy load and outdoor thermal comfort, achieving a multi-objective equilibrium, thus providing a specific workflow for similar engineering problems; (3) building performance is affected by seasonal changes—the impact of the parametric-generated building massing on energy consumption is most significant in the summer and least significant in the winter.

The multi-objective optimization design workflow developed in this study is of great significance for fine-tuned climate adaptation design in cold regions. This study uses real meteorological data from cold regions as input conditions, with a simulation duration for thermal comfort and building energy consumption covering an entire year, with time accuracy set at 365 days/year. Future research could further explore the coordination of different performance indicators (such as green health metrics, daylight comfort, building operational costs, CO_2 emissions, etc.) in multi-objective optimization design for different climate zones, such as the coordination of light and thermal environments in extremely cold regions. Additionally, the research could analyze sensitivity analysis of multiple performance indicators (e.g., the impact of building massing on outdoor thermal comfort) and quantify the extent to which various sub-indicators influence the optimization results. Further studies may also integrate machine learning techniques by training machine learning models with optimal results from multi-objective optimization design to address the long computation times associated with multi-objective optimization, thereby reducing the difficulty of using such designs.

This study's workflow proposes a multi-objective optimization design workflow for office buildings. To enhance the applicability of this workflow, corresponding performance evaluation indicators should be established for different building types (such as residential areas, schools, kindergartens, nursing homes, libraries, etc.) and design intentions (such as light comfort, carbon emissions throughout the life cycle, urban resilience, etc.). As the evaluation indicators are further refined, the multi-objective optimization of building forms will inevitably become more rational and objective, promoting the development of the construction industry toward the optimization of the urban built environment driven by big data.

The trend of using urban big data to assess the built environment is unstoppable, and human–machine collaboration is bound to develop further. Therefore, how to use the built environment evaluation system to improve the built environment in a high-quality manner is a direction that needs to be researched in the future. Future research could expand into thermal environment studies under extreme climates. Additionally, from the perspective of smart cities, real-time camera observation data can be utilized to conduct research on the correlation between building equipment and human behavior, with the aim of achieving energy saving and emission reduction through controlled building equipment. Finally, considering the perspective of healthy buildings, research can be conducted on the matching between medical data and built environment data. By studying the correlation and significance of the impact between medical data and the built environment, key points for improving the built environment can be identified.

Author Contributions: F.G.: conceptualization and investigation, S.M.: writing—original draft, S.X. and M.L.: Data processing and visualization, H.Z. and J.D.: writing—review and editing. All authors have read and agreed to the published version of the manuscript.

Funding: This research was jointly funded by the National Natural Science Foundation of China (52108044) for the project 'Study on Urban Thermal Environment Assessment and Planning Mechanism Based on Local Climate Zoning' and the Liaoning Province Social Science Federation's economic and social development project (2025lslybwzzkt-156) titled 'Research on Exploiting the Advantages of Liaoning's Marine Resources to Create Unique Tourism Products'.

Data Availability Statement: The original contributions presented in the study are included in the article, further inquiries can be directed to the corresponding authors.

Conflicts of Interest: We declare that we have no financial and personal relationships with other people or organizations that can inappropriately influence our work, and there is no professional or other personal interest of any nature or kind in any product, service, and/or company that could be construed as influencing the position presented in, or the review of, the manuscript.

References

1. Laino, E.; Iglesias, G. Extreme climate change hazards and impacts on European coastal cities: A review. *Renew. Sustain. Energy Rev.* **2023**, *184*, 113587. [CrossRef]
2. Javanroodi, K.; Mahdavinejad, M.; Nik, V. Impacts of urban morphology on reducing cooling load and increasing ventilation potential in hot-arid climate. *Appl. Energy* **2018**, *231*, 714–746. [CrossRef]
3. Kiss, B.; Szalay, Z. Modular approach to multi-objective environmental optimization of buildings. *Autom. Constr.* **2020**, *111*, 103044. [CrossRef]
4. Makki, M.; Showkatbakhsh, M.; Tabony, A.; Weistock, M. Evolutionary algorithms for generating urban morphology: Variations and multiple objectives. *Int. J. Archit. Comput.* **2018**, *17*, 147807711877723. [CrossRef]
5. Mukkavaara, J.; Shadram, F. An integrated optimization and sensitivity analysis approach to suppor t the life cycle energy trade-off in building design. *Energy Build.* **2021**, *253*, 111529. [CrossRef]
6. Ignatius, M.; Wong, N.H.; Martin, M.; Chen, S. Virtual Singapore integration with energy simulation and canopy modelling for climate assessment. *IOP Conf. Ser. Earth Environ. Sci.* **2019**, *294*, 012018. [CrossRef]
7. Safiri, S.; Nikoofard, A. Ladybug Beetle Optimization algorithm: Application for real-world problems. *J. Supercomput.* **2022**, *79*, 3511–3560. [CrossRef] [PubMed]
8. Zong, C.; Chen, X.; Deghim, F.; Staudt, J.; Geyer, P.; Lang, W. A holistic two-stage decision-making methodology for passive and active building design strategies under uncertainty. *Build. Environ.* **2024**, *251*, 111211. [CrossRef]
9. Wang, L.; Janssen, P.; Ji, G. Optimization-based design exploration of building massing typologiesd-EvoMass and a typology-oriented computational design optimization method for early-stage performance-based building massing design. *Front. Archit. Res.* **2024**, *13*, 1400–1422. [CrossRef]
10. Miao, Y.; Chen, Z.; Chen, Y.; Tao, Y. Sustainable Architecture for Future Climates: Optimizing a Library Building through Multi-Objective Design. *Buildings* **2024**, *14*, 1877. [CrossRef]
11. Delgarm, N.; Sajadi, B.; Delgarm, S. Multi-objective optimization of building energy performance and indoor thermal comfort: A new method using artificial bee colony(ABC). *Energy Build.* **2016**, *131*, 42–53. [CrossRef]
12. Xue, Q.; Wang, Z.; Chen, Q. Multi-objective optimization of building design for life cycle cost and CO_2 emissions: A case study of a low-energy residential building in a severe cold climate. *Build. Simul.* **2022**, *15*, 83–98. [CrossRef]
13. Li, J.; Wang, Y.; Xia, Y.; Song, Y.; Xie, H. Optimization of Urban Block Form by Adding New Volumes for Capacity Improvement and Solar Performance Using A Multi-Objective Genetic Algorithm: A Case Study of Nanjing. *Buildings* **2022**, *12*, 1710. [CrossRef]
14. Zhang, X.; Wang, J.; Zhou, Y.; Wang, H.; Xie, N.; Chen, D. A multi-objective optimization method for enclosed-space lighting design based on MOPSO. *Build. Environ.* **2024**, *250*, 1.1–1.15. [CrossRef]
15. Mirzabeigi, S.; Razkenari, M. Design optimization of urban typologies: A framework for evaluating building energy performance and outdoor thermal comfort. *Sustain. Cities Soc.* **2022**, *76*, 103515. [CrossRef]
16. Maksoud, A.; Alawneh, S.; Hussien, A.; Abdeen, A.; Abdalla, S. Computational Design for Multi-Optimized Geometry of Sustainable Flood-Resilient Urban Design Habitats in Indonesia. *Sustainability* **2024**, *16*, 2750. [CrossRef]
17. Khan, A.M.; Tariq, M.; Rehman, S.; Saeed, T.; Alqahtani, F.; Sherif, M. BIM Integration with XAI Using LIME and MOO for Automated Green Building Energy Performance Analysis. *Energies* **2024**, *17*, 3295. [CrossRef]
18. Zhao, J.; Guo, F.; Zhang, H.; Dong, J. Mechanisms of Non-Stationary Influence of Urban Form on the Diurnal Thermal Environment based on Machine Learning and MGWR Analysis. *Sustain. Cities Soc.* **2024**, *101*, 105194. [CrossRef]
19. Lin, H.; Ni, H.; Xiao, Y.; Zhu, X. Couple Simulations with CFD and Ladybug + Honeybee Tools for Green Façade Optimizing the Thermal Comfort in a Transitional Space in hot-humid climate. *J. Asian Archit. Build. Eng.* **2023**, *22*, 1317–1342. [CrossRef]

20. Li, Y.; Ding, J.; Zhang, Z.; Zhou, X.; Makvandi, M.; Yuan, P.; Xie, Y. Practical application of multi-material topology optimization to performance-based architectural design of an iconic building. *Compos. Struct.* **2023**, *325*, 117603. [CrossRef]
21. Noorollahi, Y.; Barabadi, P.; Taherahmadi, J.; Abbasizade, F. Multi-objective optimization of energy demand and net zero energy building design based on climatic conditions (Case study: Iran). *Int. J. Environ. Sci. Technol.* **2024**, 1–16. [CrossRef]
22. Bao, X.; Zhang, J. Multi-objective decision optimization design for building energy-saving retrofitting design based on improved grasshopper optimization algorithm. *Int. J. Renew. Energy Dev.* **2024**, *13*, 1058–1067. [CrossRef]
23. Deshpande, A.; Pagare, A.; Tomar, A. Assessing the efficacy of green building design strategies in minimizing energy consumption in commercial buildings of Mumbai: A building performance analysis. *Int. J. Sci. Res. Arch.* **2023**, *2024*, 31–39. [CrossRef]
24. Vandenbogaerde, L.; Verbeke, S.; Audenaert, A. Optimizing building energy consumption in office buildings: A review of building automation and control systems and factors influencing energy savings. *J. Build. Eng.* **2023**, *76*, 107233. [CrossRef]
25. Fu, H.; Baltazar, J.; Claridge, D. Review of developments in whole-building statistical energy consumption models for commercial buildings. *Renew. Sustain. Energy Rev.* **2021**, *147*, 111248. [CrossRef]
26. Bordas, A.; Le Masson, P.; Maxime, T.; Weil, B. What is generative in generative artificial intelligence? A design-based perspective. *Res. Eng. Des.* **2024**, 1–17. [CrossRef]
27. Fitriawijaya, A.; Jeng, T. Integrating Multimodal Generative AI and Blockchain for Enhancing Generative Design in the Early Phase of Architectural Design Process. *Buildings* **2024**, *14*, 2533. [CrossRef]
28. Liao, W.; Lu, X.; Fei, Y.; Gu, Y.; Huang, Y. Generative AI design for building structures. *Autom. Constr.* **2024**, *157*, 105187. [CrossRef]
29. Wang, H.-J.; Sun, J.; Chen, H.; Zhu, Y.L.; Zhang, Y.; Lang, X.-M.; Fan, K.; Yu, E.; Yang, S. Extreme Climate in China: Facts, Simulation and Projection. *Meteorol. Z.* **2012**, *21*, 279–304. [CrossRef]
30. Liu, Z.; Hu, L.; Chen, H.; Li, Z.; Jiang, L. Exploring the combined cooling effect of street canyon geometry and the surrounding built environment. *Environ. Sci. Pollut. Res.* **2024**, *31*, 1–18. [CrossRef]
31. Taheri, S.; Hosseini, P. Model predictive control of heating, ventilation, and air conditioning (HVAC) systems: A state-of-the-art review. *J. Build. Eng.* **2022**, *60*, 105067. [CrossRef]
32. Arvidsson, R.; Tillman, A.-M.; Sandén, B.; Janssen, M.; Nordelöf, A.; Kushnir, D.; Molander, S. Environmental Assessment of Emerging Technologies: Recommendations for Prospective LCA: Prospective LCA. *J. Ind. Ecol.* **2018**, *22*, 1286–1294. [CrossRef]
33. Potrc Obrecht, T.; Röck, M.; Hoxha, E.; Passer, A. BIM and LCA integration: A systematic literature review. *Sustainability* **2020**, *12*, 5534. [CrossRef]
34. Luo, X.; Du, L. Energy consumption simulations of rural residential buildings considering differences in energy use behavior among family members. *Build. Simul.* **2024**, *17*, 1335–1358. [CrossRef]
35. Ao, J.; Du, C.; Jing, M.; Li, B.; Chen, Z. A Method of Integrating Air Conditioning Usage Models to Building Simulations for Predicting Residential Cooling Energy Consumption. *Buildings* **2024**, *14*, 2026. [CrossRef]
36. Bai, C.; Liu, J. Prediction and Management of Building Energy Consumption Based on Building Environment Simulation Design Platform DeST and Meteorological Data Analysis Algorithm. *Strateg. Plan. Energy Environ.* **2024**, *43*, 357–380. [CrossRef]
37. *GB55015-2021*; General Code for Energy Efficiency and Renewable Energy Application in Buildings. Standardization Administration of China: Beijing, China, 2021.
38. Höppe, P. Different aspects of assessing indoor and outdoor thermal comfort. *Energy Build.* **2002**, *34*, 661–665. [CrossRef]
39. Lai, D.; Guo, D.; Hou, Y.; Lin, C.; Chen, Q. Studies of Outdoor Thermal Comfort in Northern China. *Build. Environ.* **2014**, *77*, 110–118. [CrossRef]
40. Coccolo, S.; Kämpf, J.; Scartezzini, J.-L.; Pearlmutter, D. Outdoor human comfort and thermal stress: A comprehensive review on models and standards. *Urban Clim.* **2016**, *18*, 33–57. [CrossRef]
41. Xi, T.; Li, Q.; Mochida, A.; Meng, Q. Study on the outdoor thermal environment and thermal comfort around campus clusters in subtropical urban areas. *Build. Environ.* **2012**, *52*, 162–170. [CrossRef]
42. Ibrahim, Y.; Kershaw, T.; Shepherd, P. A methodology For Modelling Microclimates: A Ladybug-tools and ENVI-met verification study. In Proceedings of the 35th PLEA Conference Sustainable Architecture and Urban Design: Planning Post Carbon Cities, A Coruña, Spain, 1–3 September 2020.
43. Ibrahim, Y.; Kershaw, T.; Shepherd, P. Improvement of the Ladybug-tools microclimate workflow: A verification study. In Proceedings of the IBPSA-England Building Simulation and Optimisation Conference 2020, Loughborough, UK, 21–22 September 2020.
44. Sun, R.; Chen, D.; Xu, Y.; Lai, D.; Liu, W. Improving outdoor thermal comfort of a kindergarten by optimizing its building shape with genetic algorithm. *E3S Web Conf.* **2023**, *396*, 05011. [CrossRef]
45. Sadeghipour Roudsari, M.; Pak, M. Ladybug: A parametric environmental plugin for grasshopper to help designers create an environmentally-conscious design. In Proceedings of the BS 2013: 13th Conference of the International Building Performance Simulation Association, Chambery, France, 25–28 August 2013; pp. 3128–3135.
46. *ANSI/ASHRAE Standard 55*; Thermal Environmental Conditions for Human Occupancy. ASHRAE (American Society of Heating, Refrigerating and Air-Conditioning Engineers): Atlanta, GA, USA, 2021.

47. Karl, F.; Pielok, T.; Moosbauer, J.; Pfisterer, F.; Coors, S.; Binder, M.; Schneider, L.; Thomas, J.; Richter, J.; Lang, M.; et al. Multi-Objective Hyperparameter Optimization in Machine Learning—An Overview. *ACM Trans. Evol. Learn. Optim.* **2023**, *3*, 1–50. [CrossRef]
48. Guo, W.; Dong, Y. Enhancing energy-efficient building design: A multi-agent-assisted MOEA/D approach for multi-objective optimization. *Energy Inform.* **2024**, *7*, 102. [CrossRef]
49. Wang, L.; Janssen, P.; Stouffs, R. Teaching Computational Design Optimization—An experimental course for performance-based building massing exploration. In Proceedings of the 41st Conference on Education and Research in Computer Aided Architectural Design in Europe, eCAADe 2023, Graz, Austria, 20–22 September 2023; pp. 179–188.
50. Ji, Y.; Xu, M.; Zhang, T.; He, Y. Intelligent Parametric Optimization of Building Atrium Design: A Case Study for a Sustainable and Comfortable Environment. *Sustainability* **2023**, *15*, 4362. [CrossRef]
51. Wang, L. Workflow for applying optimization-based design exploration to early-stage architectural design—Case study based on EvoMass. *Int. J. Archit. Comput.* **2022**, *20*, 41–60. [CrossRef]
52. Zhang, Y.; Teoh, B.K.; Zhang, L. Multi-objective optimization for energy-efficient building design considering urban heat island effects. *Appl. Energy* **2024**, *376*, 124117. [CrossRef]
53. Li, M.; Wang, Z.; Chang, H.; Wang, Z.; Guo, J. A novel multi-objective generative design approach for sustainable building using multi-task learning (ANN) integration. *Appl. Energy* **2024**, *376*, 124220. [CrossRef]
54. Li, L.; Qi, Z.; Qingsong, M.; Gao, W.; Wei, X. Evolving multi-objective optimization framework for early-stage building design: Improving energy efficiency, daylighting, view quality, and thermal comfort. *Build. Simul.* **2024**, *17*, 2097–2123. [CrossRef]